Denoising of Image Corrupted by Additive-Impulsive Noise using Sparse Representation

Volodymyr Ponomaryov, and Alfredo Palacios-Enriquez

Abstract—In this paper, a novel framework is presented for suppression of noise in a color image contaminated by a mixture of additive and impulsive noise. This method consists of three principal stages: in the first stage, the suppression of impulsive noise is performed where the corrupted by impulsive noise pixels should be detected and filtered by a variant of median filter. In the second stage, novel additive noise suppression filter is used on Wavelet domain applying the sparse representation and 3D-filtering. Finally, the image obtained on the previous filtering stages is processed to correct non-desirable effects such as fine details blurring and texture distortions. Evaluation of novel approach in suppressing complex noise has been performed using objective criteria (PSNR and SSIM) and subjective perception via human visual system confirming their better performance in comparison with state-of-the-art techniques.

Keywords—Image Denoising, Additive Noise, Impulsive Noise, Mixed Noise,Sparse Representation, PSNR,SSIM.

I. INTRODUCTION

The fundamental problem in image processing consists in reducing a noise while preserving the most of image features. The presence of random digital noise in an image reduces the performance of digital systems, so the noise can be considered such an undesirable signal that adheres to objects of interest in digital image. Research is ongoing to develop filters capable to suppress different types of noise in order to obtain an image sufficiently similar to original one. Principal difficulties in any filtering technique are that a processing procedure should perform suppression of a noise meanwhile the fine details, edges, and texture properties can be saved unchanged. If fine characteristics of an image are distorted during filtering, these drawbacks could cause economic impact, misinterpretation during medical diagnosis, incorrect classification of objects in the satellite images, erroneous detection of obstacles by autonomous robots, errors in telemedicine applications, etc. [1].

During image acquisition, additive noise may be present, and during its transmission or acquisition, further contamination may be caused by impulsive noise. These two types of noise are the most common but are not the only types. Images may be corrupted by interference and imperfections in the channel or the reception equipment. Additionally, digital cameras can introduce noise because of failure in their sensor CCD, electronic interference or errors in data acquisition [2].

V. Ponomaryov and A. Palacios-Enriquez are with the Instituto Politcnico Nacional (Mexico) Av. Santa Ana 951, San Francisco Culhuacan, C.P 09080, Ciudad de Mexico. e-mails: vponomar@ipn.mx and alfredoepe@yahoo.com.mx

Impulsive noise in an image appears as spots that can range in size from very large to very small. There are several models of contamination by impulsive noise: impulsive noise with fixed value and impulsive noise with random distribution. In practice, the most common type of noise in a digital image is additive noise, which is generally assumed to be a stochastic Gaussian process with a zero mean and a known variance of σ^2. In most cases, it is spatially independent. In corruption by additive noise, all pixels in an image are corrupted; however, the pixels can be recovered by subtracting the additive random error.

These two types of noise are the most common but are not the only types [3]. The most common model of mixed noise used is a combination of additive noise (usually, Gaussian one) and impulsive noise. This type of noise can be represented as follows:

$$E(i,j) = \begin{cases} e(i,j) + n_{add} & \text{, with probability } 1 - p_k \\ n_{imp} & \text{, with probability } p_k \end{cases}, \quad (1)$$

where $e(i,j)$ is the original image, n_{add} is a random process with Gaussian probability density $N(0,\sigma^2)$, n_{imp} is modelled via uniform probability distribution, and $E(i,j)$ is the noisy image.

II. RELATED WORKS

The restoration of corrupted images by a mixture of additive and impulsive noise requires new techniques, since existing techniques that are developed in additive noise suppression are not capable of eliminating artefacts produced by impulsive noise.

There are several filtering techniques for Gaussian additive noise elimination, among them, there exist different techniques based on search of a group of pixels called as *reference block*. Jain [4] proposed a technique, in which WT is applied to some neighbourhoods or patches with a specified degree of similarity. Filtering is performed for each sub-band wavelet by obtaining a threshold that adapts to the conditions of each a neighbourhood. Lukin [5] proposed an adaptive filter based on an assessment of the image locality for filtering by DCT to obtain a neighbourhood and to estimate the local variance; then, the variance is used to distinguish homogeneous and heterogeneous areas. Finally, the threshold depending on the area in question is set. Bahoura [6] proposed a signal denoising technique based on wavelet that consists of applying a thresholding function to the wavelet coefficients.

Jin [7] introduced new non-local operators to interpret the filter as a regularization of the Dirichlet's functional. These operators are used to propose a new non-local model H^1. Smoothing and fidelity are derived from the same geometric principle. Experiments show that non-local operators produce a good interpretation of the NLM filter. Buades [8] proposed a new method for measuring noise and comparing performance of the methods in removing image noise. Then, the authors proposed a new algorithm based on NLM for a nonlocal average of all pixels in an image.

Dabov [9] presented the video filtering method VBM3D based on a highly dispersed signal in the local domain of a 3D transform. This method uses a 3D array called group that is applied to store all blocks similar to the block being processed. The grouping is performed by searching for similar blocks in the space-time domain. For each a 3D group, filtering and shrinkage is performed in the 3D transform domain. In our previous study [10], we performed similar to BM3D framework (*SM3D-DCTNS*) using DCT and block matching procedures that demonstrated superior performance in comparison with NML and BM3D techniques. One drawback appears in this kind of filtering is that the found similarity measure may cause the impulses that can be considered as fine details, so the corrupted pixel is not filtered.

There are several papers that use ideas of fuzzy logic theory in denoising and can suppress additive or impulsive noise in separated form [11] [12] [13]. For example, in our previous study [12], two frameworks (FMANS_2 and FMANS_H) have been designed to suppress additive Gaussian noise but any of these techniques has no ability in filtering complex (impulsive-additive) noise.

Techniques for additive noise do not perform a correct restoration of pixels contaminated by impulsive noise, so it is necessary to restore such pixels before restoring the pixels that are contaminated by additive noise. There are different techniques for the elimination of impulsive noise, where the detection of noisy pixels or random impulses is performed during the first stage, following these impulses should be suppressed during filtering process.

Different techniques for the elimination of impulsive noise are mostly based on use of kind of median filter or their multichannel modification such as Vector Median Filter [14], Switching Median Filter [15], etc. Other techniques are based on the detection of contaminated pixels in the first step, and then a filtering process should be only applied to corrupted pixels.

Xu [16] proposed an efficient filter for universal impulse noise removal. This method consists of two stages: impulse detection and filtering. For detection, a robust local image statistic, called the extremum compression rank-order absolute difference (ECROAD), is designed to detect impulse noise in an image. For filtering, the universal impulse noise filter is proposed by combining the ECROAD statistic with the non-local means.

Nasri [17] presented an effective filtering method to remove impulse noise from images. In this two-stage method, the detected noise-free pixels remain unchanged. Then, a Gaussian filter with adaptive variances according to the image noise level is applied to the noisy pixels. Veerakumar [18] introduced an adaptive radial basis function interpolation-based impulse noise removal algorithm. This approach consists of two stages: noisy pixel detection and correction. The radial basis function interpolation scheme is used to estimate the unknown noisy pixel value from the noise-free known neighboring pixel values. For both noisy pixel detection and correction, a center sliding window is considered at each a pixel location.

The methods described above are designed for a specific, additive or impulsive type of noise. There are several novel techniques that can remove a mixture of noises, usually additive noise and impulsive noise. Most of these techniques perform the filtering of impulsive noise in a first stage, and the filtering of additive noise is applied during second stage.

In [19, 20], suppression techniques for mixed noise (additive Gaussian and impulsive saturated) are proposed, in which the detection and filtering of impulsive noise are employed first, and the suppression of additive Gaussian noise occurs in a second stage.

In [19], the impulsive noise detector is based on the differences between a central pixel and its neighbours. When a contaminated pixel is detected, it is replaced by a mean of all neighbours. Filtering of additive Gaussian noise is performed using a bilateral filter (BF),in which the parameters of BF are adjusted based on an estimation of local variance. Jiang [21] proposed a method to suppress mixed noise called weighted encoding with sparse nonlocal regularization (WESNR). The WESNR technique does not use a detector of impulses as an individual stage, so each corrupted block is encoded over a pre-learned dictionary to remove the impulse noise and additive white Gaussian noise simultaneously in a soft impulse pixel detection manner. The suppression of mixed noise is performed by weighting the encoding residual in such a way that the final encoding residual will tend to follow a Gaussian distribution. The weighted encoding and sparse nonlocal regularization are unified into a variational framework, which is easy to minimize.

In this work, novel technique of suppressing a mixture of additive and impulsive noise is developed. The suppression of mixed noise is divided in several stages: the suppression of impulsive noise is performed using a detector of impulses and a variant of median filter; the additive noise suppression is performed on wavelet domain that in difference with our previous study (Palacios-Enriquez, 2016) demonstrates better quality, employing the advantage of sparse representation; and, finally, in order to improve the quality of the image, obtained during the previous suppression stages, a post-processing stage should be applied.

III. Proposed method

The proposed method to filter image corrupted by impulsive-additive noise using Sparse Representation and 3D Wavelet Filtering (**FMN-3DWT-C**) can be described in three stages: a) impulse noise detection and filtering, b) additive noise filtering, and c) post-processing procedure (See Fig. 1). In the following sections, each a step will be described.

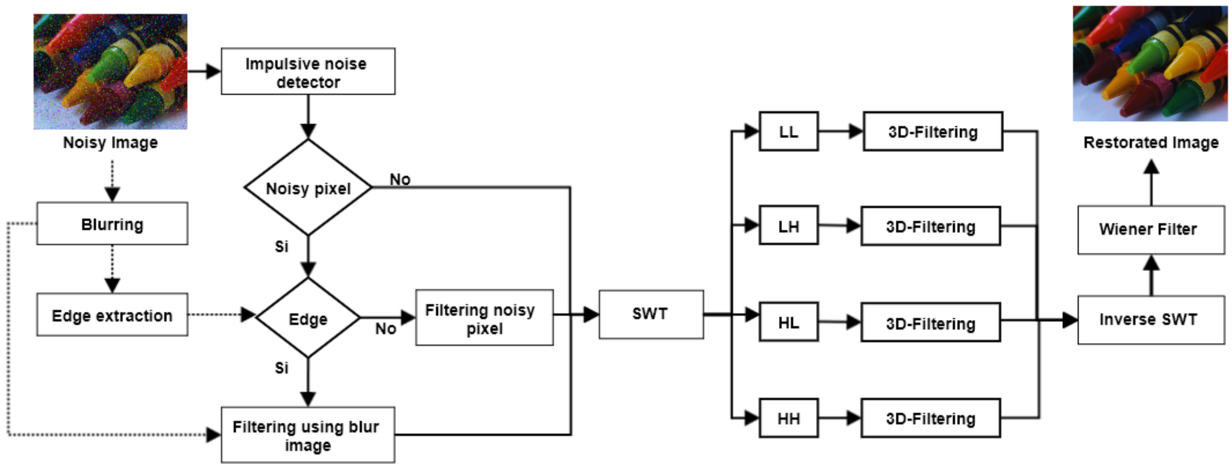

Fig. 1. Block-diagram of proposed method FIAN-3DW.

A. Impulsive Noise Suppression

In developed impulsive noise suppression stage, the detection and restoring of pixels contaminated by impulsive noise are performed.

1) Fuzzy Impulsive Noise Detector: Detection of noisy pixels is a very important stage because a poor detection could generate undesirable effects, such as: blurring in areas of fine details or texture distortion.

The detection process in current framework is based on gradient value and fuzzy sets theory. In this stage, all pixels are analyzed using a vicinity of 3×3 pixels, where several neighbors are assigned to a choosen direction (Northwest (NW), North (N), Northeast (NE), East (E), Southeast (SE), South (S), Southwest (SW), West (W)).

The basic gradient value in direction (k, l) of a central pixel in the position (i, j) is defined as follows:

$$\nabla_{(k,l)} E(i,j) = E(i+k, j+l) - E(i,j), \tag{2}$$

where $k, l \in \{-1, 0, 1\}$ and (k, l) belong to one of eight directions. It is necessary distinguish between corrupted and edge pixels, two values are defined, and they are known as related gradients. These values are calculated by using neighboring pixels that form a right angle in the same direction as the basic gradient (see Fig. 2(b)).

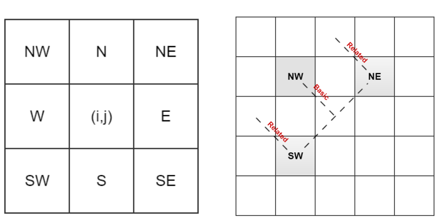

(a) Vicinity of a central pixel. (b) Gradients related to the NW direction.

Fig. 2. Vicinity of 3×3 to calculate basic and related gradients.

The next step consists of defining a fuzzy gradient in each a direction to distinguish between a noisy pixel and a noise-free pixel. The fuzzy gradient value $\nabla_R^F A(i,j)$ for direction R is defined as follows:

$$\begin{aligned}
&\textbf{IF}\ [\\
&|\nabla_R E(i,j)|\ is\, large\ \textbf{AND}\ |\nabla'_R E(i,j)|\ is\, small\ \textbf{OR}\\
&|\nabla_R E(i,j)|\ is\, large\ \textbf{AND}\ |\nabla''_R E(i,j)|\ is\, small\ \textbf{OR}\\
&\nabla_R E(i,j)\ is\, big\, positive\ \textbf{AND}\ \nabla'_R E(i,j)\ \textbf{AND}\\
&\nabla''_R E(i,j)\ are\, big\, negative\ \textbf{OR}\\
&\nabla_R E(i,j)\ is\, big\, negative\ \textbf{AND}\ \nabla'_R E(i,j)\ \textbf{AND}\\
&\nabla''_R E(i,j)\ are\, big\, positive\,]\\
&\textbf{THEN}\\
&\nabla_R^F E(i,j)\ is\, large,
\end{aligned}$$

where $\nabla_R E(i,j)$ is the basic gradient and, $\nabla'_R E(i,j)$ and $\nabla''_R E(i,j)$ are the related gradients connected with a given direction $R = \{NW, N, NE, E, SE, S, SW, W\}$. In order to determine whether a central pixel is contaminated by impulsive noise, the following fuzzy rule is used:

$$\begin{aligned}
&\textbf{IF}\ most\, of\, the\, eight\ \nabla_R^F E(i,j)\ are\, large\\
&\textbf{THEN}\ the\, central\, pixel\ E(i,j)\ is\, an\, impulse\, noise\, pixel.
\end{aligned}$$

In particular, if four or more fuzzy gradients are large, then the analyzed pixel is tagged as a noisy pixel. The detection of random spikes impulses is performed on each a pixel. If a pixel is detected as a corrupted one, then their position is tagged, thus generating an image as a map of the corrupted pixels.

2) Restoration of pixels corrupted by impulsive noise: The restoration of corrupted pixels is realized for each channel RGB of independent form. Let explain below the process for channel R. Once, that all impulses in the image are identified and tagged, the next step consist of replacing the noisy pixels using filtering technique. In the filtering of pixels contaminated by impulsive noise, the information generated by the impulsive noise detector is used. Each a pixel is analyzed to know if a noisy pixel exists in its position. In the detection of impulses process, it can not be avoided that some pixels, that belong to edges and /or textures, are detected as noisy pixels. So, it is necessary to include additional information to correct this fact.

The edge extraction techniques of an image are based in changes of intensity within a neighborhood, so that the impulses could be detected as a edge. In order to extract the edges of an image contaminated by mixed noise, two steps have been proposed:

1) Blurring the image contaminated by mixed noise.
2) Edges extraction.

Firstly, the blurring of noisy image is performed using a median filter with a vicinity of 5×5 pixels. Finally, the edges extraction is performed using the proposed technique by Canny et. al. [**?**]. This process is shown in figure 2.

(a) Noisy image. (b) Blur image. (c) Edges channel R.

Fig. 3. Edge extraction process for an image contaminated with mixed noise.

First, if the position (i, j) is found a tagged as a noisy pixel, following a neighborhood W of size 3×3 pixels is taken. Then, the restoration of the pixel is performed considering whether the pixel belongs to an edge or not.

First case. The pixel does not belong to an edge.
The restoration stage of corrupted pixel is based on the Median Filter vector (VMF) proposed by Astola [22] and is only applied to those pixels that are marked as noisy ones.

Firstly, the sum of absolute differences ($SAD(i, j)$) of each a pixel with its neighbors is performed. The value $SAD(i, j)$ is defined as:

$$SAD_{i,j} = \sum_{k=1}^{3}\sum_{l=1}^{3} |W(i, j) - W(k, l)| \tag{3}$$

where (i, j) is the position of pixel, and (k, l) are the positions of their neighbors. From this process nine values are obtained, as shown in figure 4.

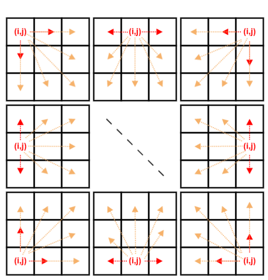

Fig. 4. Obtaining of value $SAD_{i,j}$.

It should be mentioned that the values tagged as noisy pixels that in the neighborhood are not considered in the sum of absolute differences. So, the value of the pixel is estimated as follows:

$$\widehat{E}_{NotEdge}(i, j) = W(r, s), \tag{4}$$

Second case. The pixel belongs to an edge.
When a pixel belongs to an edge, it does not imply that it is not contaminated by impulsive noise, so we obtain a first approximation $\widehat{E}_1(i, j)$, considering that the pixel does not belong to an edge (Eq. 4).

$$\widehat{E}_1(i, j) = \widehat{E}_{NotEdge}(i, j) = W(r, s). \tag{5}$$

Next, a vicinity $W_{blur}(i, j)$ from the blur image is taken and a second approximation is obtained as follows:

$$\widehat{E}_2(i, j) = median\{W_{blur}(k, l)\} \quad \forall\ k, l = 1, 2, 3, \tag{6}$$

The restoration of pixel is defined as:

$$\widehat{E}_{Edge}(i, j) = \frac{\widehat{E}_1(i, j) + \widehat{E}_2(i, j)}{2} \tag{7}$$

B. Additive Noise Filtering

The additive noise filtering is based on sparse representation and 3D filtering on Wavelet Transform domain. The techniques that use sparse representation to suppress additive noise are based in the behavior of noise in the domain of some fixed bases like: Fourier, Cosine, Wavelet, etc. Further, the filtering based on shrinkage method allows reducing the additive noise, whereas the edges and fine details suffer less deterioration when such reconstruction is performed [23].

The proposed additive noise filtering stage is performed on WT domain and can be divided in two stages: 1) grouping using block-matching, and 2) 3D-filtering.

1) Wavelet Domain: The Wavelet Transform (WT) has an important role in the image processing. Four sub-bands, called Low-Low (LL), Low High (LH), High-Low (HL) and High-High (HH), are obtained when the WT process is applied.

Next, the additive noise suppression is performed to each a sub-band in independent form. The additive noise suppression stage is performed in Wavelet domain where there should be applied two processing procedures: 1) grouping using block-matching, and 2) 3D-filtering. The figure 5 explains the process of additive noise suppression on WT domain.

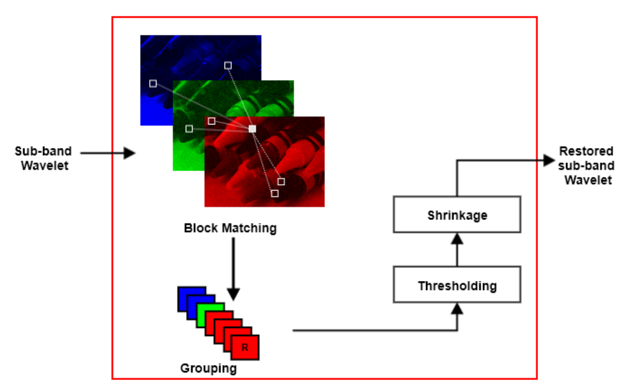

Fig. 5. Filtering process to each sub-band Wavelet.

Grouping via block-matching: The performing the procedure of block matching is realized using the three channels of color, the highly similar blocks to a reference block should be located, and these ones are stored in a structure called group. It is necessary to note that the blocks are 2D arrays and the grouping process [9] is formed as a 3D array.

The similarity degree between two blocks is obtained employing a similarity measure. If the similarity is higher than a chosen threshold, the block can be considered as similar one and it enters to a current group. In this framework, the sum absolute difference (SAD) is used as matching criterion, which is written as follows:

$$SAD(p,q) = \sum_{m=1}^{M}\sum_{n=1}^{N} |E(p,q) - E(p+m,q+n)|, \quad (8)$$

where M and N are the image dimensions, and $E(p,q)$ is the reference block in the position (p,q). Let denote the reference block as $A(p,q)$, and then all similar blocks are $A_r(p,q)$.

3D filtering: The designed 3D filtering uses two processes: thresholding and shrinkage. In the thresholding, all wavelet coefficients that belong to each a block of the 3D array are compared with a fixed threshold (t_h). If the absolute value of a coefficient is less or equal to the threshold, this coefficient is replaced with the zero value, as follows:

$$\widehat{E}_{3D}(p,q,r) = \begin{cases} 0 & , |E_{3D}(p,q,r)| \leq t_h \\ E_{3D}(p,q,r) & , \text{otherwise} \end{cases}. \quad (9)$$

In the next step, there is performed the shrinkage of the 3D array, i.e., from the 3D array, there should be obtain an approximation of the 2D array. This can be performed using an averaging filter with chosen weights that depend on similarity grade, as follows:

$$\widehat{E}(i,j) = \frac{\sum_{l=1}^{k} E_l(i,j) w_l}{\sum_{l=1}^{k} w_l} \quad (10)$$

where w_k are the weights that are defined as follow:

$$w_k = 1 - SAD(E_1(i,j), E_k(i,j)). \quad (11)$$

Finally, in order to obtain a filtered image $\widehat{Y}(i,j)$, the additive noise filtering is applied to each RGB channel of an image.

C. Post-processing

In the previous filtering stages are produced some artefacts undesirables, so in the filtered image such artefacts should be corrected. A Wiener filter [24] is employed to increase the quality of filtered image as follows:

$$\widehat{Y}_{Wiener}(i,j) = \mu + \frac{\sigma_W^2 - v^2}{\sigma_W^2}\left[\widehat{Y}(i,j) - \mu\right], \quad (12)$$

where μ is the local mean, σ_W^2 is the local variance and v^2 is the average of all the local estimated variances.

IV. Experimental result

The experiment results were performed using a set of color test images proposed by Malinski [25] shown in figure 6. Mentioned set contains images with different texture and fine details structure that can guarantee robustness of investigating techniques.

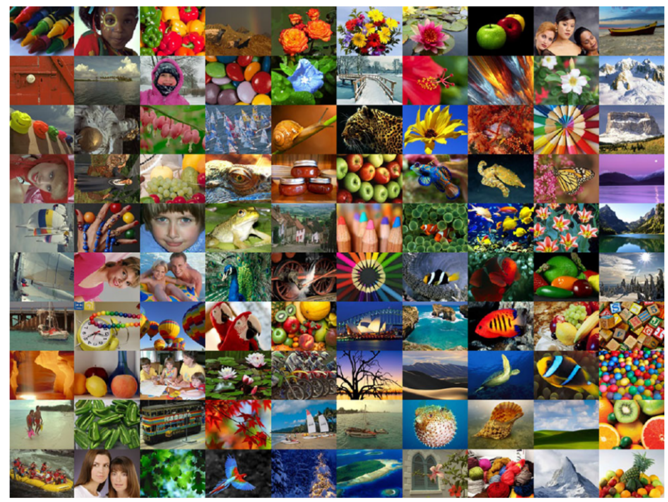

Fig. 6. Database proposed by Malinski.

A. Evaluation criteria

The evaluation criteria used to characterize performance are the peak signal-to-noise ratio (PSNR) and structural similarity index measure (SSIM). The PSNR is an objective criterion measurement and is defined as follows:

$$PSNR = 10log_{10}\left(\frac{255^2}{MSE}\right), \quad (13)$$

where the *Mean Square Error* (MSE) is calculated as:

$$MSE = \frac{1}{MN}\sum_{x=0}^{M-1}\sum_{y=0}^{N-1}\left[\widehat{E}(x,y) - E(x,y)\right]^2. \quad (14)$$

The SSIM captures human perception and this measure was introduced in [26] and it is defined as:

$$SSIM(x,y) = [l(x,y)]^{\alpha} \cdot [c(x,y)]^{\beta} \cdot [s(x,y)]^{\gamma} \quad (15)$$

where $\alpha = \beta = \gamma = 1$.

B. Efficiency of the proposed filter

The experimental results (PSNR, SSIM) for all test images are shown in Table I. Additionally, we use the subjective visual perception presenting filtered images and their error images for the best state-of-the art filters to compare their noise suppression.

TABLE I
THE AVERAGE PSNR AND SSIM VALUES.

%	10	20	30	40	50
σ			**PSNR**		
10	34.33	33.52	31.95	28.51	24.30
20	29.43	28.76	27.43	25.21	22.12
30	25.61	25.15	24.16	22.60	20.29
40	23.17	22.72	21.94	20.66	18.80
50	21.36	20.95	20.27	19.14	17.54
σ			**SSIM**		
10	0.9873	0.9844	0.9745	0.9365	0.8592
20	0.9428	0.9343	0.9119	0.8699	0.7958
30	0.8754	0.8648	0.8416	0.8008	0.7335
40	0.8192	0.8054	0.7795	0.7394	0.6733
50	0.7682	0.7535	0.7262	0.6832	0.6204

1) Comparison with state-of-art techniques: There are different techniques for mixed noise suppression. In order to evaluate the proposed method, we compare with the better existing state-of-art techniques: Wiener [24], Bilateral [19], NLM [8] and WESNR [21]. The filter Wiener, Bilateral and NLM were designed to decrease the additive noise, so it is necessary to perform, previously, the filtering of impulsive noise to compare with our technique.

In figures 7, 8, 9 and 10 there are shown the visual results obtained to images: *pic002*, *pic029*, *pic059* and *pic084* corrupted by different values of % and σ in the case of impulsive and additive noise, respectively.

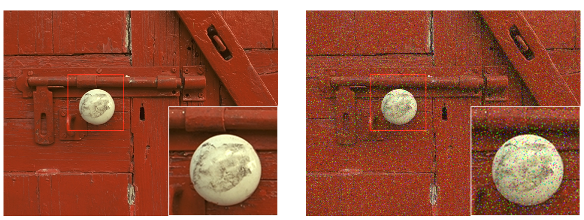

(a) Original image. (b) Noisy image.

(c) Bilateral. (d) Bilateral Error. (e) Wiener. (f) Wiener Error.

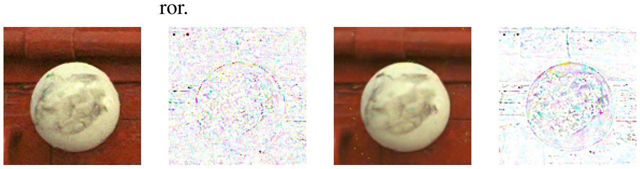

(g) NLM. (h) NLM Error. (i) WESNR. (j) WESNR Error.

(k) FMN-3DWT-C. (l) FMN-3DWT-C Error.

Fig. 7. Inverted error images (amplified by 5) of the image *pic002* filtered by Bilateral, Wiener, NLM, WESNR and FMN-3DWT-C techniques for a mixture of noise of Additive Noise ($\sigma = 10$) and Random Impulsive Noise ($\% = 10$).

(a) Original image. (b) Noisy image.

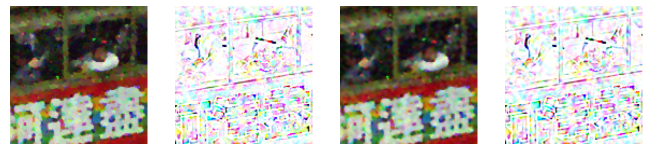

(c) Bilateral. (d) Bilateral Error. (e) Wiener. (f) Wiener Error.

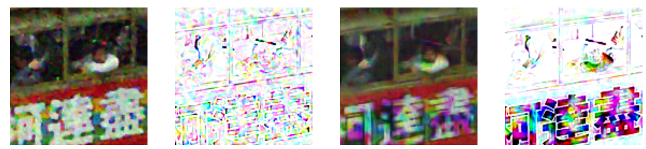

(g) NLM. (h) NLM Error. (i) WESNR. (j) WESNR Error.

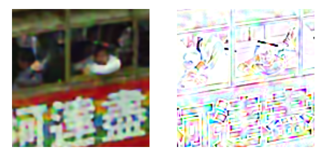

(k) FMN-3DWT-C. (l) FMN-3DWT-C Error.

Fig. 8. Inverted error images (amplified by 3) of the image *pic029* filtered by Bilateral, Wiener, NLM, WESNR and FMN-3DWT-C techniques for a mixture of noise of Additive Noise ($\sigma = 30$) and Random Impulsive Noise ($\% = 30$).

Also, the criterias values(PSNR, SSIM and MAE) for images presented in figures 7, 8, 9 and 10 are shown in table II.

TABLE II
THE PSNR, MAE AND SSIM VALUES OBTAINED TO IMAGES: PIC002, PIC029, AND PIC059.

			PSNR		
	Bilateral	Wiener	NLM	WESNR	FMN-3DWT-C
pic002	30.13	30.65	29.41	29.66	**32.33**
pic029	21.96	22.29	22.12	21.36	**24.19**
pic059	19.55	19.82	19.91	13.90	**21.96**
pic084	17.10	17.65	17.72	11.84	**20.02**
			SSIM		
	Bilateral	Wiener	NLM	WESNR	FMN-3DWT-C
pic002	0.9834	0.9856	0.9811	0.9808	**0.9904**
pic029	0.6265	0.6473	0.6411	0.6970	**0.7986**
pic059	0.5008	0.5205	0.5276	0.4282	**0.6674**
pic084	0.64013	0.67131	0.67821	0.45768	**0.8019**

V. CONCLUSION

A novel filtering method to suppress a mixture of additive noise and impulsive noise is presented. The denoising approach consists of three principal stages: impulsive noise suppression, additive noise suppression and post-processing. The experimental results demonstrate that our proposal exhibits better processing performance than state-of-the-art techniques in suppressing mixed noise with varying texture characteristics

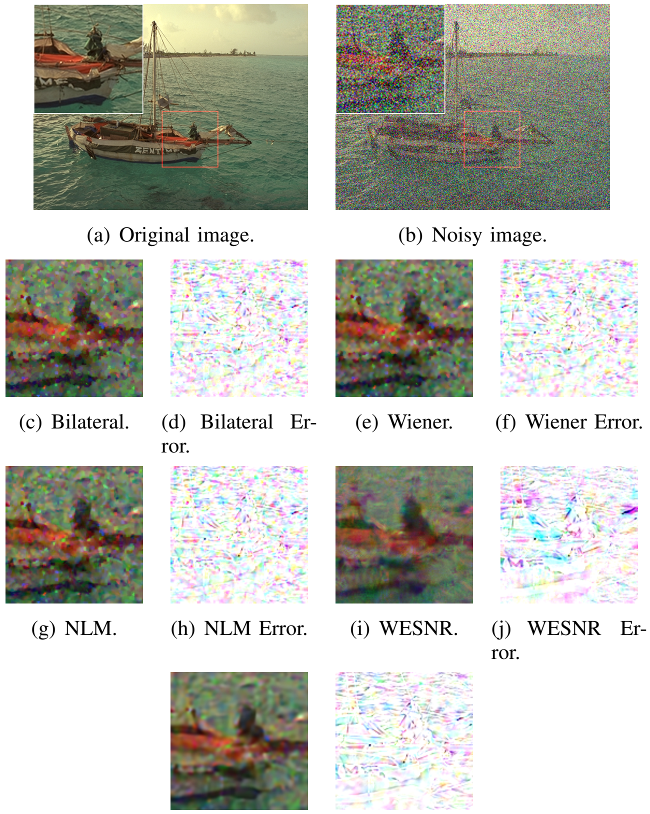

(a) Original image. (b) Noisy image.

(c) Bilateral. (d) Bilateral Error. (e) Wiener. (f) Wiener Error.

(g) NLM. (h) NLM Error. (i) WESNR. (j) WESNR Error.

(k) FMN-3DWT-C. (l) FMN-3DWT-C Error.

Fig. 9. Inverted error images (amplified by 2) of the image *pic059* filtered by Bilateral, Wiener, NLM, WESNR and FMN-3DWT-C techniques for a mixture of noise of Additive Noise ($\sigma = 40$) and Random Impulsive Noise ($\% = 40$).

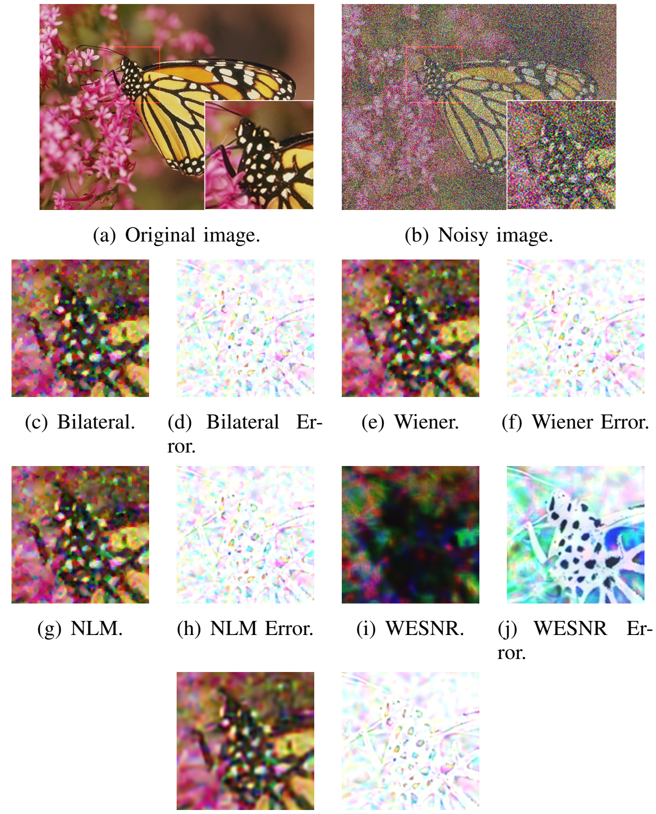

(a) Original image. (b) Noisy image.

(c) Bilateral. (d) Bilateral Error. (e) Wiener. (f) Wiener Error.

(g) NLM. (h) NLM Error. (i) WESNR. (j) WESNR Error.

(k) FMN-3DWT-C. (l) FMN-3DWT-C Error.

Fig. 10. Inverted error images of the image *pic084* filtered by Bilateral, Wiener, NLM, WESNR and FMN-3DWT-C techniques for a mixture of noise of Additive Noise ($\sigma = 50$) and Random Impulsive Noise ($\% = 50$).

and edges. Future work should be devoted to implementing the current filtering approach to restore video.

ACKNOWLEDGMENT

Authors would like to thank to Instituto Politecnico Nacional (Mexico) and Consejo Nacional de Ciencia y Tecnologia (Mexico) (grant 220347) for their support in realizing this work.

REFERENCES

[1] I. Pitas, *Digital image processing algorithms and applications*. Wiley, 2000.

[2] I. Young, J. Gerbrands, and L. Vliet, *Fundamentals of image processing*. TU Delft, Faculty of Applied Physics, Pattern Recognition Group, 1995.

[3] I. T. Young, J. J. Gerbrands, and L. J. van Vliet, *Fundamentals of Image Processing (v.2.3)*. Delft University of Technology, 2007.

[4] P. Jain and V. Tyagi, "LAPB: Locally adaptive patch-based wavelet domain edge-preserving image denoising," *Information Sciences*, vol. 294, no. October, pp. 164–181, 2015.

[5] V. Lukin, D. Fevralev, and O. Pogrebnyak, "Nonstationary noise locally adaptive filtering in DCT domain," *Congress (WAC), 2012*, pp. 1–6, 2012.

[6] M. Bahoura and H. Ezzaidi, "FPGA-Implementation of Discrete Wavelet Transform with Application to Signal Denoising," *Circuits, Systems, and Signal Processing*, vol. 31, no. 3, pp. 987–1015, jun 2012. [Online]. Available: http://link.springer.com/10.1007/s00034-011-9355-0

[7] Y. Jin, J. Jost, and G. Wang, "A New Nonlocal H 1 Model for Image Denoising," *Journal of Mathematical Imaging and Vision*, vol. 48, no. 1, pp. 93–105, jan 2014. [Online]. Available: http://link.springer.com/10.1007/s10851-012-0395-2

[8] A. Buades and B. Coll, "A non-local algorithm for image denoising," *Computer Vision and Pattern*, vol. 2, no. 0, pp. 60–65, 2005.

[9] K. Dabov, A. Foi, V. Katkovnik, and K. Egiazarian, "Image Denoising by Sparse 3-D Transform-Domain Collaborative Filtering," *IEEE Transactions on Image Processing*, vol. 16, no. 8, pp. 2080–2095, aug 2007. [Online]. Available: http://ieeexplore.ieee.org/document/4271520/

[10] A. Palacios-Enriquez and V. Ponomaryov, "Image Denoising using Block Matching and Discrete Cosine Transform with Edge Restoring," *IEEE Conference Proceedings. Conielecomp*, vol. 978-1-5090, pp. 140–147, 2016.

[11] T. Mélange, M. Nachtegael, S. Schulte, and E. E. Kerre,

"A fuzzy filter for the removal of random impulse noise in image sequences," *Image and Vision Computing*, vol. 29, no. 6, pp. 407–419, 2011.

[12] V. I. Ponomaryov, H. Montenegro-Monroy, F. Gallegos-Funes, O. Pogrebnyak, and S. Sadovnychiy, "Fuzzy color video filtering technique for sequences corrupted by additive Gaussian noise," *Neurocomputing*, vol. 155, pp. 225–246, 2015.

[13] A. J. Rosales-Silva, F. J. Gallegos-Funes, and V. I. Ponomaryov, "Fuzzy Directional (FD) Filter for impulsive noise reduction in colour video sequences," *Journal of Visual Communication and Image Representation*, vol. 23, no. 1, pp. 143–149, 2012.

[14] R. Lukac, "Adaptive vector median filtering," *Pattern Recognition Letters*, vol. 24, no. 12, pp. 1889–1899, 2003.

[15] P. E. Ng and K. K. Ma, "A switching median filter with boundary discriminative noise detection for extremely corrupted images," *IEEE Transactions on Image Processing*, vol. 15, no. 6, pp. 1506–1516, jun 2006. [Online]. Available: http://ieeexplore.ieee.org/document/1632204/

[16] G. Xu and J. Tan, "A Universal Impulse Noise Filter with an Impulse Detector and Nonlocal Means," *Circuits, Systems, and Signal Processing*, vol. 33, no. 2, pp. 421–435, feb 2014. [Online]. Available: http://link.springer.com/10.1007/s00034-013-9640-1

[17] M. Nasri, S. Saryazdi, and H. Nezamabadi-pour, "A Fast Adaptive Salt and Pepper Noise Reduction Method in Images," *Circuits, Systems, and Signal Processing*, vol. 32, no. 4, pp. 1839–1857, aug 2013. [Online]. Available: http://link.springer.com/10.1007/s00034-012-9546-3

[18] T. Veerakumar, R. P. K. Jagannath, B. N. Subudhi, and S. Esakkirajan, "Impulse Noise Removal Using Adaptive Radial Basis Function Interpolation," *Circuits, Systems, and Signal Processing*, pp. 1–32, jun 2016. [Online]. Available: http://dx.doi.org/10.1007/s00034-016-0352-1

[19] Y. Zhang, X. Tian, and P. Ren, "An adaptive bilateral filter based framework for image denoising," *Neurocomputing*, vol. 140, pp. 299–316, 2014.

[20] I. R. Terol-Villalobos and J. D. Mendiola-Santibañez, "Filtering of mixed Gaussian and impulsive noise using morphological contrast detectors," *IET Image Processing*, vol. 8, no. 3, pp. 131–141, mar 2014. [Online]. Available: http://digital-library.theiet.org/content/journals/10.1049/iet-ipr.2012.0615

[21] Jielin Jiang, Lei Zhang, and Jian Yang, "Mixed Noise Removal by Weighted Encoding With Sparse Nonlocal Regularization," *IEEE Transactions on Image Processing*, vol. 23, no. 6, pp. 2651–2662, jun 2014. [Online]. Available: http://ieeexplore.ieee.org/document/6800039/

[22] J. Astola, P. Haavisto, and Y. Neuvo, "Vector median filters," *Proceedings of the IEEE*, vol. 78, no. 4, pp. 678–689, apr 1990. [Online]. Available: http://ieeexplore.ieee.org/document/54807/

[23] A. M. Bruckstein, D. L. Donoho, and M. Elad, "From Sparse Solutions of Systems of Equations to Sparse Modeling of Signals and Images," *SIAM Review*, vol. 51, no. 1, pp. 34–81, feb 2009. [Online]. Available: http://epubs.siam.org/doi/10.1137/060657704

[24] J. S. Lim, *Two-dimensional signal and image processing*. Prentice Hall, 1990.

[25] L. Malinski and B. Smolka, "Fast adaptive switching technique of impulsive noise removal in color images," *Journal of Real-Time Image Processing*, pp. 1–22, may 2016. [Online]. Available: http://link.springer.com/10.1007/s11554-016-0599-6

[26] Z. Wang, A. C. Bovik, H. R. Sheikh, S. Member, E. P. Simoncelli, and S. Member, "Image Quality Assessment : From Error Visibility to Structural Similarity," vol. 13, no. 4, pp. 600–612, 2004.

Volodymyr Ponomaryov received the Ph.D. degree in 1974 and D.Sci. in 1981. His research interests include signal/image/video processing, pattern recognition, and real-time filtering. He has also been a promoter of 38 Ph.D.s. He has published of about 500 international scientific and conference papers, and also 23 patents of ex USSR, Russia and Mexico, and five scientific books.

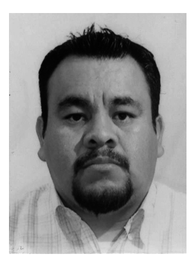

Alfredo Palacios-Enriquez received the Ph.D. degree in Communications and electronics from the National Polytechnic Institute of Mexico in 2018. His research interests include image/video processing, denoising, and real-time processing.